Redox Biology 71 (2024) 103102

Contents lists available at ScienceDirect

Redox Biology

journal homepage: www.elsevier.com/locate/redox

Identification of tyrosine brominated extracellular matrix proteins in normal and fibrotic lung tissues

Litiele Cezar Cruz [a,b], Aida Habibovic [b], Bianca Dempsey [a], Mariana P. Massafera [a], Yvonne M. W. Janssen-Heininger [b], Miao-chong Joy Lin [b], Evan T. Hoffman [c], Daniel J. Weiss [c], Steven K. Huang [d], Albert van der Vliet [b,**], Flavia C. Meotti [a,*]

[a] Department of Biochemistry, Institute of Chemistry, University of São Paulo, SP, Brazil
[b] Department of Pathology and Laboratory Medicine, Larner College of Medicine, University of Vermont, VT, USA
[c] Department of Medicine, Larner College of Medicine, University of Vermont, Burlington, VT, USA
[d] Department of Internal Medicine, University of Michigan Medical School, Ann Arbor, MI, USA

ARTICLE INFO

Keywords:
Peroxidasin
Hypobromous acid
Bromotyrosine
Laminin
Collagen
Tubulointerstitial nephritis antigen-like 1
Pulmonary fibrosis

ABSTRACT

Peroxidasin (PXDN) is a secreted heme peroxidase that catalyzes the oxidative crosslinking of collagen IV within the extracellular matrix (ECM) via intermediate hypobromous acid (HOBr) synthesis from hydrogen peroxide and bromide, but recent findings have also suggested alternative ECM protein modifications by PXDN, including incorporation of bromide into tyrosine residues. In this work, we sought to identify the major target proteins for tyrosine bromination by HOBr or by PXDN-mediated oxidation in ECM from mouse teratocarcinoma PFHR9 cells. We detected 61 bromotyrosine (BrY)-containing peptides representing 23 proteins in HOBr-modified ECM from PFHR9 cells, among which laminins displayed the most prominent bromotyrosine incorporation. Moreover, we also found that laminin α1, laminin β1, and tubulointerstitial nephritis antigen-like (TINAGL1) contained BrY in untreated PFHR9 cells, which depended on PXDN. We extended these analyses to lung tissues from both healthy mice and mice with experimental lung fibrosis, and in lung tissues obtained from human subjects. Analysis of ECM-enriched mouse lung tissue extracts showed that 83 ECM proteins were elevated in bleomycin-induced fibrosis, which included various collagens and laminins, and PXDN. Similarly, mRNA and protein expression of PXDN and laminin α/β1 were enhanced in fibrotic mouse lung tissues, and also in mouse bone-marrow-derived macrophages or human fibroblasts stimulated with transforming growth factor β1, a profibrotic growth factor. We identified 11 BrY-containing ECM proteins, including collagen IV α2, collagen VI α1, TINAGL1, and various laminins, in both healthy and mouse fibrotic lung tissues, although the relative extent of tyrosine bromination of laminins was not significantly increased during fibrosis. Finally, we also identified 7 BrY-containing ECM proteins in human lung tissues, again including collagen IV α2, collagen VI α1, and TINAGL1. Altogether, this work demonstrates the presence of several bromotyrosine-modified ECM proteins, likely involving PXDN, even in normal lung tissues, suggesting a potential biological function for these modifications.

1. Introduction

The extracellular matrix (ECM) forms a complex mixture comprising the interstitial matrix and basement membranes (BM), and performs vital functions for cellular support, intercellular communications, and regulation of tissue development. The BM is a specialized structure directly underlying epithelial, endothelial, and muscle cells, and forms a thin, continuous layer composed primarily of collagen IV and laminins [1]. It plays crucial roles in regulating cellular processes, such as cell signaling, growth, differentiation, migration, and cell adhesion, and its self-organization is essential for appropriate intercellular interactions and organ development and function. One recently identified

* Corresponding author. Department of Biochemistry, Institute of Chemistry (IQUSP), University of São Paulo, Av. Prof Lineu Prestes 748, São Paulo, SP, 05508-0000, Brazil.
** Corresponding author. Department of Pathology and Laboratory Medicine, Larner College of Medicine, University of Vermont, 149 Beaumont Avenue, Burlington, VT, 05405, USA.
E-mail addresses: albert.van-der-vliet@med.uvm.edu (A. van der Vliet), flaviam@iq.usp.br (F.C. Meotti).

https://doi.org/10.1016/j.redox.2024.103102
Received 13 January 2024; Received in revised form 17 February 2024; Accepted 21 February 2024
Available online 23 February 2024

BM-associated enzyme that plays an important role in ECM modeling is peroxidasin (PXDN), a heme peroxidase expressed and secreted by several cell types [2]. PXDN utilizes hydrogen peroxide (H_2O_2) to catalyze the oxidation of bromide (Br^-) to generate hypobromous acid (HOBr), which in turn oxidizes specific methionine and hydroxylysine/lysine residues within the C-terminal non-collagenous (NC1) domains of two adjacent collagen IV protomers to form covalent sulfilimine bonds between collagen IV molecules, to help generate a collagenous network and provide structural integrity to the BM [2,3]. This unique role for Br^- in oxidative collagen IV crosslinking forms the first evidence for the essential role of bromine in living organisms. More recent studies have demonstrated the incorporation of bromine into BM proteins via PXDN, including the formation of bromotyrosine in ECM proteins, indicating an alternative PXDN-oxidative mechanism unrelated to collagen IV crosslinks [4,5].

Although enzymatic halogenation of biological molecules, such as polynucleotides, peptides, and proteins, is widespread in nature, particularly by diverse haloperoxidases in algae, sponges, bacteria and fungi, its biological importance in mammalian organisms is much less appreciated [6,7]. The best known physiological mammalian halogenation involves the iodination of tyrosine by thyroid peroxidase (TPO) to form thyroid hormones [8], with important function in regulation of metabolism. Other mammalian halogenation events include chlorination or bromination of tyrosines by myeloperoxidase or eosinophil peroxidase during inflammatory disease, which are considered diagnostic oxidative biomarkers of ongoing inflammation, although they may also impact on cellular properties during disease conditions [9,10]. In light of the biological importance of PXDN for ECM biology [11], and the recently observed increases in PXDN in cardiovascular disorders [12–15], various cancers [16–18], and fibrotic diseases [19–21], it is plausible that the physiological or pathological functions of PXDN may in part be mediated by halogenation of proteins.

The present study was conducted to identify ECM proteins that are subject to bromination by PXDN. Since the amino acid tyrosine is the major target for oxidative halogenation in proteins, resulting in formation of stable adducts [22], we focused our efforts on identifying protein targets for PXDN-mediated bromotyrosine (BrY) or dibromotyrosine (2BrY) formation. Secondly, we extended our analyses to lung tissues from mice or humans, and based on presumed increases in PXDN during fibrotic lung disease, also to lung tissues from mice with experimentally-induced fibrosis and from human specimens diagnosed with idiopathic pulmonary fibrosis. Indeed, we identified several BM proteins that were brominated on specific tyrosine residues, most notably isoforms of collagen IV, collagen VI, tubulointerstitial nephritis antigen-1, and various laminins, in ECM from cultured carcinoma cells, and from normal murine or human lung tissues, suggesting a potential physiological function of such bromination events. Moreover, we also observed tyrosine bromination of these and other ECM/BM proteins in fibrotic lung tissues, associated with increased overall expression of PXDN and many ECM proteins.

2. Experimental procedures

2.1. PFHR9 culture, ECM enrichment, and treatments

PFHR9 (ATCC CRL-2423), an epithelial cell line from mouse embryonal carcinoma, was maintained in high glucose DMEM (Dulbecco's Modified Eagle's Medium) containing 10% fetal bovine serum (FBS), streptomycin (100 mg/mL) and penicillin (30 mg/mL) at 37 °C in a 5% CO_2 atmosphere. PFHR9 cells were cultured in complete DMEM medium until confluence, after which medium was changed daily with complete medium for 6 days to allow ECM deposition, in the presence or absence of 50 μM PHG (phloroglucinol, a PXDN inhibitor). After ECM deposition, cells were washed twice with PBS (10 mM, pH 7.4) and scraped/lysed with 1% sodium deoxycholate, 1 mM EDTA in 50 mM Tris-HCl pH 8.0 and 1X protease inhibitors (Sigma COEDTAF-RO), sonicated (~3–6 times for 20 s at 20% power, followed by 30 s resting on ice, to reduce viscosity) and spun (20,000×*g* for 20 min). The precipitated ECM was washed three times with 1 M NaCl in 10 mM Tris-HCl pH 7.5 and 1X protease inhibitors (Sigma COEDTAF-RO). Then, ECM was suspended in PBS (10 mM, pH 7.4) and sonicated again to homogenize. Protein was quantified and 100 μg protein homogenate was treated with 100 μM HOBr, or with 100 μM H_2O_2 plus 100 μM NaBr, in PBS (10 mM, pH 7.4) for 90 min with regular mixing (every 10 min) with a pipette to avoid protein agglomeration. The reaction was stopped by adding 1% azide. Reagent concentrations were based on previous similar studies [5,23]. HOBr was prepared by adding an equal volume of 0.25 M HOCl to 1.5 M NaBr in 0.1 M NaOH while vortexing. After 10 min, HOBr concentration was determined by measuring its absorbance at 329 nm with $\varepsilon_{HOBr} = 335\ M^{-1}cm^{-1}$ [24] after 1:100 dilution in PBS. Stock solutions were diluted in PBS and we verified that final dilutions in the ECM reaction mixture did not alter pH.

2.2. Mouse model of bleomycin-induced lung fibrosis

Mice C57BL/6NJ (Strain #:005304, Jackson Laboratories, ME, USA) were bred in-house under pathogen-free conditions with constant room temperature and humidity and a 12 h light cycle. Mice from both sexes were fed ad libitum with a formulated diet (Prolab IsoPro RMH 3000 - 5P76) for up to 3 months prior to experimentation. Mice were subjected to 50 μL PBS (10 mM, pH 7.4) or bleomycin (2.5 U/kg - Teva Pharmaceutical USA 0703-3155-01) by oropharyngeal administration under isofluorane anesthesia [25]. Ten animals per group were randomized by gender. Bleomycin instillation induces alveolar epithelial injury which typically results in the development of lung fibrosis after 2–4 weeks. After 21 days, mice were euthanized by i.p. pentobarbital (NDC-76478-501-50) and lung tissues were harvested for biochemical and histological analyses. The superior and post-caval lobes from the right lung tissue were used for RNA extraction. Inferior and middle lobes were used for protein analysis. For proteomic analysis, 50–100 μg of each lung tissue was homogenized with 1% sodium deoxycholate, 1 mM EDTA in 50 mM Tris-HCl pH 8.0 and 1X protease inhibitors (Thermo Fisher Scientific 78442) using bead beaters and a TissueLyser (QIAGEN). Samples were then sonicated as described above. ECM from lung tissues was more fibrous and difficult to homogenize, and we excluded non-homogenized pieces for proteomic sample preparations. The left lungs were collected for paraffin-embedding and immunohistochemistry analysis. All studies involving mice were approved by the Institutional Animal Care and Use Committee (protocol # PROT0202000078).

2.3. Bone marrow-derived macrophages (BMDM) and human primary lung fibroblasts (HLF)

Bone marrow was flushed from the femurs and tibias of euthanized mice and suspended in complete RPMI medium containing 10% fetal bovine serum (FBS), streptomycin (100 mg/mL), penicillin (30 mg/mL) and 5 ng/mL M-CSF (R&D Systems 416-ML/CF) overnight at 37°C in a 5% CO_2 atmosphere. The following day, non-adherent cells were collected, washed in PBS (10 mM, pH 7.4), and contaminating red blood cells were lysed by briefly resuspending pelleted cells in water. The remaining cells were then differentiated into BMDMs by culturing in complete RPMI containing 30 ng/mL M-CSF for 7 days. HLF (ATCC PCS-201-013) were cultured in fibroblast basal medium (ATCC PCS-201-030) with fibroblast growth kit-low serum (ATCC PCS-201-041) at 37 °C in a 5% CO_2 atmosphere. A total of 5×10^5 BMDMs or 1×10^6 HLFs were treated in a 24 or 6-well plate, respectively, with 5 ng/mL TGF-β1 (R&D Systems 7666-MB/CF) in their respective culture medium for 48 h. For experiments involving immunohistochemical staining, BMDMs were seeded in chamber slides (Millipore PEZGS0816) at 4×10^4 cells/well and treated as described above.

2.4. Human lung tissues

Postmortem lung tissues from human subjects with a diagnosis of usual interstitial pneumonia rendered by a board-certified pathologist were provided by the autopsy suite at the University of Vermont Medical Center, and were processed immediately upon receipt within a time frame of 4 h after autopsy and processed within 24 h post mortem. Lung tissue was rinsed in sterile PBS, blotted, flash-frozen in liquid nitrogen and stored at −80 °C until analysis. These samples were determined to constitute non-human subject research by the UVM Institutional Review Board (CHRMS: M13-306). In addition, non-involved human lung tissues were also provided from lungs rejected for transplantation at the University of Michigan Medical School and provided by Dr. Huang, and processed and frozen similarly. Aliquots of frozen lung tissue sections were processed to generate ECM-enriched extracts for proteomics analysis as described above for mouse lung tissues. In addition, we also reanalyzed proteome datasets from a recent study of decellularized postmortem human lung tissues from non-diseased subjects or subjects with IPF, which had been dissected into diverse anatomical regions for analysis of regional lung ECM proteomes [26].

2.5. Proteomic analysis

2.5.1. In-solution digestion

Ten (10) μg of ECM homogenate from each sample was first incubated in 100 mM ammonium bicarbonate with 8 M urea and 6 M guanidine hydrochloride and reduced in 9.1 mM DTT for 1 h at 37 °C based on a previous protocol [27]. Then, samples were alkylated with 33.9 mM iodoacetamide for 30 min, reduced again with 4 mM DTT for 15 min, and digested with PNGase F Glycan Cleavage Kit according to manufacturer protocol (Gibco - A39245) for 1 h, all at 37 °C. Next, samples were digested with Sequencing Grade Modified Trypsin (Promega V5111), at a protein/trypsin ratio 40:1 w/w, for 2 h at 37°C. A second aliquot of trypsin (40:1 w/w) was added and samples were incubated overnight at 37°C constant shaking. After acidification with trifluoroacetic acid (final concentration 1% v/v), the ECM digests were desalted using the StageTip protocol in case of PFHR9 cell studies [28] or using peptide desalting spin columns (Thermo Fisher Scientific 89852) in case of lung tissues analyses. Samples were dried and stored at −80 °C until MS analyses.

2.5.2. Data-dependent acquisition (DDA) and parallel reaction monitoring (PRM) proteomics

Digested and desalted ECM from PFHR9 cell studies were resuspended in 0.1% formic acid for MS analyses. An Easy-nLC 1200 UHPLC (Thermo Scientific, Bremen, Germany) was used for peptide separation with a linear gradient of solvent A (0.1% formic acid) and solvent B (80% acetonitrile in 0.1% formic acid). Each sample was loaded onto a trap column (Acclaim PepMap 100, C18, 3 μm, 75 μm × 2 cm, nanoViper, Thermo Scientific) with 20 μL (or 12 μL for PRM) of solvent A at 500 bar. After this period, the trapped peptides were eluted onto a C18 column (Acclaim PepMap RSLC, C18, 2 μm, 75 μm × 15 cm, nanoViper, Thermo Scientific) at a flow rate of 300 nL/min. Peptides were eluted from the column using a linear gradient of 5–28% B for 80 min (43 min for PRM) followed by a linear gradient of 28–40% B for 10 min (3 min for PRM). Finally, the percentage of solvent B was increased to 95% in 2 min and the column was washed for 12 min with this solvent proportion. Re-equilibration of the system with 100% A was performed before each injection. Samples were analyzed on an Orbitrap Fusion Lumos mass spectrometer (Thermo Scientific, Bremen, Germany) using a nanospray Flex NG ion source (Thermo Scientific, Bremen, Germany), and operating in positive ESI mode with the capillary temperature at 300 °C, and S-Lens RF level at 30%. A full MS scan was followed by data-dependent acquisition (DDA) or PRM MS^2 scans. Both MS and MS^2 scans were performed in the Orbitrap analyzer. Precursor ions selected for MS^2 on DDA were excluded for subsequent MS^2 scans for 40s. Precursor ions were fragmented by higher-energy c-trap dissociation (HCD) with a normalized collision energy of 30%. In DDA, the resolution for the full scan mode was set as 120,000 (at *m/z* 200), and the automatic gain control (AGC) target at 5×10^5. The *m/z* range 350–1550 was monitored. For accurate mass measurements, the lock mass option was enabled in the MS scan and the polydimethylcyclosiloxane ions (*m/z* = 445.12003) were used for internal calibration in real-time. Each full scan was followed by a data-dependent MS^2 acquisition with a resolution of 30,000 (at *m/z* 200), a maximum fill time of 54 ms, and an isolation window of 1.2 *m/z*. In PRM experiments, a full mass spectrum at 120,000 resolution relative to *m/z* 200 (AGC target 4×10^5, 50 ms maximum injection time, *m/z* 200–1600) was followed by PRM scans at 60,000 resolution (AGC target 5×10^4, 118 ms maximum injection time, 1.2 *m/z* isolation window) as triggered by an inclusion list. The Advanced Peak Determination (APD) algorithm was applied for improved precursor identification. Ion activation/dissociation was performed at a normalized collision energy of 30% in HCD collision cell. For accurate mass measurements, RunStart EASY-IC™ option was enabled for mass calibration prior to each PRM run.

Digested and desalted ECM from mouse or human lung tissue samples were suspended in 2.5% formic acid and 2.5% acetonitrile and analyzed on an Orbitrap Eclipse mass spectrometer coupled to an EASY-nLC 1200 system (Thermo Fisher Scientific). Samples were first analyzed by data-dependent acquisition (DDA). Digests were loaded onto a 100 μm i. d. capillary column packed with UChrom C18 (1.8 μm particle size, 120 Å, Cat. No: PN-80001; Nanolcms, CA) at a flow rate of 300 nL/min. The column end was laser pulled to a ~3 μm orifice and packed with minimal amounts of 5 μm Magic C18AQ before packing with the 1.8 μm particle size chromatographic materials. Peptides were separated by a solvent system composed of solvent A: 100% water/0.1% formic acid and solvent B: 80% acetonitrile/0.1% formic acid and nanosprayed at 1.9 kV into the Eclipse through the Flex™ Ion Source with the ion transfer tube set at 275 °C. For DDA, the following gradients were used: 5–25% B in 110 min, 25–40% B over 25 min, 40–95% B in 25 min and then 95% B for 4 min, followed by an immediate return to 5% B in 1 min and a hold at 100% A for 15 min before the next injection. Mass spectrometry data were acquired in a data-dependent "Top speed in 3 s - high load" acquisition mode, in which a survey scan from *m/z* 375–1500 at 60,000 resolution (RF Lens (%) = 30; AGC target = Standard; max IT = Auto; profile mode, microscan = 1) was followed by higher-energy collisional dissociation (HCD) tandem mass spectrometry (MS/MS) scans on the most abundant ions at 15,000 resolution (AGC target = standard; max IT = AUTO; centroid mode). MS/MS scans were acquired after quadrupole isolation with an isolation width of 1.6 *m/z* and a (fix) normalized collisional energy of 30%. Dynamic exclusion was enabled (exclude after 1 time; low and high mass tolerance of 10 ppm; exclusion duration: 60 s). Expected LC Peak Width = 30 s. Lock mass function was not activated. PRM was carried out to quantify brominated laminin peptides of interest with alternating MS and targeted MS/MS (tMS^2) scans (2 scan groups/experiments) using a shorter 60-min gradient of 0–25% B in 20 min, 25–40%B in 10 min, 40–95%B in 10 min, 95% B for 9 min, followed by an immediate return to 5% B in 1 min and 5% B in 10 min. Full scans were acquired from *m/z* 300-2000 at 60,000 resolution (RF Lens = 30%; microscan = 1; AGC target = Standard; max IT = Auto; profile mode). The precursor masses of various CS were imported into the inclusion list. Precursors of interest were isolated by quadruple and collision-induced dissociation (CID) was utilized to produce sufficient coverage of b- and y-ions, which were detected in the Orbitrap at 7500 resolution in centroid mode, with the following settings: AGC target = Standard; max IT = Auto; isolation width of 1.6 *m/z*; and a normalized collisional energy of 30%. Expected LC Peak Width = 15 s. Internal lock mass function was not activated.

2.5.3. Protein and modified peptides identifications

Tandem mass (MS/MS) spectra were searched against UniProt (www.uniprot.org), *Mus musculus* or *Homo sapiens* database of March 2023,

using the MaxQuant software search engine v. 2.3.1.0 (Max Planck Institute of Biochemistry, Martinsried, BY, German) or Proteome Discoverer v. 2.5 software (Thermo Fisher Scientific, Waltham, MA, USA) from monoisotopic mass with fixed modification of carbamidomethylation on cysteine (+57.0214 Da) and variable modifications of oxidation on methionine (+15.9949 Da), deamidation on asparagine (+0.9840 Da), acetylation on N-terminal (+42.0105 Da) and bromination/dibromination on tyrosine (+77.9105 or +155.8210 Da). MaxQuant and Proteome Discoverer default mass tolerance was used for precursor (10 ppm) and product ions (0.02 Da). Two missed cleavages and a minimum of two peptides per protein with at least one unique peptide by identification were allowed. Similar search criteria were used to reanalyze previously reported proteomics analysis of ECM fractions from decellularized lung tissues by Hoffman et al. [26]. The DDA results were normalized by label-free quantification (LFQ) and protein statistical difference accessed using Perseus software v. 2.0.10.0 (Max Planck Institute of Biochemistry, Martinsried, BY, German). PRM ion products intensities were quantified by area peak integrations on Skyline software v. 23.0.9.187 (MacCoss Lab, Seattle, WA, USA) using the DDA data (cell or mouse tissue) to build the library. Panther (www.pantherdb.org) was used to identify the cellular component (Gene Ontology enrichment). Extracellular proteins were considered following the Panther divisions as basement membrane, extracellular matrix, extracellular region, or extracellular space, and for each protein, the classification was double-checked manually on Uniprot (www.uniprot.org).

2.6. qRT-PCR

RNA was extracted from mouse tissue, BMDMs, or HLFs using RNeasy Micro Kit (QIAGEN 74004) according to manufacturer protocol, and samples were homogenized using metal beads in a TissueLyser (QIAGEN). The cDNA was prepared using the High Capacity RNA-to-cDNA Kit (Thermo Fisher Scientific 4388950) according to manufacturer's protocol. Quantitative RT-PCR was performed using iQ Sybr Green supermix (Bio-Rad) according to manufacturer's protocol. SYBR fluorescence was analyzed by a CFX Real-Time PCR Detection System (Bio-Rad). Primers were obtained from Invitrogen, and primer sequences are listed in Supplemental Table 1. Results were calculated by the $2^{-\Delta\Delta CT}$ method and expressed as relative mRNA expression.

2.7. Western blot

Lung tissues or cell samples were homogenized using metal beads and TissueLyser (QIAGEN) on ice in RIPA Buffer (50 mM Tris/HCl, pH 7.5, 150 mM NaCl, 1% NP-40, 0.1% SDS, 0.5% sodium deoxycholate) containing Protease Inhibitor Cocktail (Thermo Fisher Scientific 78442). Total protein content was measured by the BCA method (Thermo Fisher Scientific 23225), and 20–50 μg protein was separated on a 4–20% reducing SDS-polyacrylamide (Bio-rad 5671094) gel and transferred to a polyvinylidene difluoride (PVDF) membrane. Membranes were incubated with a mouse (monoclonal 1:1000) or human (polyclonal 1:2000) PXDN primary antibody (both provided by Dr. Miklos Geiszt at Semmelweis University, Hungary and verified using PXDN-deficient mice or cells [29]) overnight and subsequently incubated for 1 h with secondary antibody conjugated with HRP and visualized by enhanced chemiluminescence (PI32106). Actin was used as a housekeeping protein to normalize protein load. Quantification of the signals were performed using ImageJ software (NIH, Bethesda, MD, USA).

2.8. Immunofluorescence analysis

The left mouse lungs were fixed in 4% PFA, paraffin-embedded, and cut in 5-μm sections using a microtome (Leica 2030 BIOCUT Manual), and deparaffinized. Then, tissues were blocked for 1 h in 10% NGS (Gibco PCN5000), 1% BSA (Gibco 15260037), and 0.1% Tx-100 (Sigma-Aldrich T9284) in PBS (10 mM, pH 7.4). BMDMs on chamber slides were fixed in 4% PFA, permeabilized with 0.3% of Triton, and blocked with 2% BSA. Tissues and cells were then stained overnight with anti-laminin α1/β1 antibody (R&D Systems MAB4656, 1:50 in blocking solution). Then, slides were washed several times and incubated with an Alexa Fluor 647 (Invitrogen A21247, 1:500) secondary antibody and DAPI (Invitrogen D1306, 10 μg/ml) in blocking solution. Slides were covered using Aqua-Poly (Polyscience 18606-20) and imaged using a Nikon A1R Confocal microscope. Fluorescence was analyzed at Cy5 mode with an excitation peak at 651 nm and an emission peak at 670 nm. Tissue sections were analyzed at 20x, and cells were analyzed at 40x, and fluorescence intensity was quantified in selected parenchymal regions or positively stained cells using Halo software (Indica Labs, Albuquerque, NM, USA).

2.9. Statistical analysis

All data are expressed as mean ± standard error of the mean (SEM). Differences among groups were evaluated by Student's T-test and were considered significant when $p < 0.05$. DDA protein statistical difference in Heatmap also used the Permutation-based False Discovery Rate (FDR) method. All analyses were performed using GraphPad Prism v.10 (GraphPad Software, San Diego, CA, USA).

3. Results

3.1. HOBr and PXDN mediate tyrosine bromination in ECM proteins from PFHR9 cells

We first analyzed enriched ECM from PFHR9 cells for the presence of bromotyrosine (BrY)-modified proteins after treatment with either HOBr or H_2O_2/NaBr. In total, we identified 61 modified peptides representing 23 proteins, five of which had different sites of cleavage (Table 1). Representative MS with isotope distributions and MS^2 spectra are shown in Supplemental Fig. 1. Laminin subunits α1, β1, and γ1 represented the highest amount of bromotyrosine modifications with 32 different tyrosine site targets. Brominated tyrosines in laminins comprised 52% of the total number of BrY-modified peptides identified in ECM from PFHR9. Laminin α1 contains 96 tyrosine residues and 13% of them were HOBr-targeted. Similarly, laminin β1 has 57 tyrosines with 19% being brominated, and laminin γ1 with 46 tyrosines had 20% brominated. Two recent studies have similarly addressed tyrosine chlorination [23] and nitration [30] of laminin-111 by myeloperoxidase (MPO). The detected BrY modifications in our study largely matched chlorinated tyrosines (69%) or nitrated tyrosines (85%) in laminin α1 in these prior studies. Similarly, for laminin β1, 45% and 64% of brominated tyrosine sites matched identified chlorination sites and nitration sites, respectively. For laminin γ1, 11% and 78% of bromination events matched the chlorination and nitration sites, respectively. In general, these comparisons indicate that multiple tyrosine sites in laminins are susceptible to halogenation, and that bromination site preference is more similar to nitration than chlorination. Other BM proteins such as collagen IV, perlecan, nidogen-2, secreted protein acidic and rich in cysteine (Sparc), 40S ribosomal protein SA (laminin cell surface receptor), and tubulointerstitial nephritis antigen-like (Tinagl1), also were tyrosine brominated by HOBr.

Compared to the large number of tyrosine brominated peptides observed by addition of HOBr, only 4 BrY-containing peptides could be detected in the H_2O_2/NaBr treatment group (Table 1), which likely reflects more selective and site-specific bromination by secreted PXDN, the only haloperoxidase that was detectable in ECM from these cells (Supplementary Table 2). To address this, we used target monitoring to quantify BrY-modified peptides from ECM of PHFR9 cells in the absence or presence of phloroglucinol (PHG, a PXDN inhibitor) (Fig. 1). Analysis of BrY-modified or corresponding unmodified peptides from laminin α1 (Fig. 1A) or Tinagl1 (Fig. 1B) showed that tyrosine bromination occurred on about 2.5 and 5% of total tyrosines, respectively, and was in

Table 1
HOBr and PXDN mediate bromination of ECM proteins from PFHR9 cells. Peptides with bromotyrosine (3-Br-Tyr) and/or di-bromotyrosine (3,5-Br-Tyr) were identified by data dependent acquisition mass spectrometry (DDA-MS).

Protein	Peptide	*m/z*	Variable modifications	Bromide Sites	Identified groups
14-3-3 protein sigma – Sfn	NLLSVA**Y**K	493.22127	Bromination (Y)	Y^{48}	HOBr
40S ribosomal protein AS – Rpsa	**Y**VDIAIPCNNK	692.78189	Bromination (Y)	Y^{156}	HOBr
Basement membrane-specific heparan sulfate proteoglycan core protein (Perlecan) - Hspg2	AFA**Y**LQVPER	636.27456	Bromination (Y)	Y^{2976}	HOBr
	TCESLGAGG**Y**R	624.71929	Bromination (Y)	Y^{1636}	HOBr
Calreticulin – Calr	HEQNIDCGGG**Y**VK	777.7857	Bromination (Y)	Y^{109}	HOBr
	VHVIFN**Y**K	366.49745	Bromination (Y)	Y^{150}	HOBr
Cell migration-inducing and hyaluronan-binding protein - Cemip	LVQ**Y**LNAVPDGR	711.82241	Bromination (Y)	Y^{222}	HOBr
	NAGISDCTATA**Y**PR	787.7988	Bromination (Y)	Y^{1182}	HOBr
	VITEDS**Y**PGYIPKPR	604.94373	Bromination (Y)	Y^{656}	HOBr
Cofilin-1 - Cfl1	NIILEEGKEILVGDVGQTVDDP**Y**TTFVK	1057.5096	Bromination (Y)	Y^{68}	HOBr
Collagen alpha-1(IV) chain - Col4a1	ND**Y**SYWLSTPEPMPMSMAPISGDNIRPFISR	1217.5299	Bromination (Y)	Y^{1519}	HOBr
Collagen alpha-2(IV) chain - Col4a2	GTCH**Y**FANK	588.20054	Bromination (Y)	Y^{1662}	HOBr
Connective tissue growth fator - Ctgf	TAVGPALAA**Y**R	584.26145	Bromination (Y)	Y^{181}	HOBr
Endoplasmic reticulum chaperone BiP - Hspa5	ITPS**Y**VAFTPEGER	822.84882	Bromination (Y)	Y^{66}	HOBr
	MKETAEA**Y**LGKK	482.88141	Bromination (Y)	Y^{161}	HOBr
Endoplasmin - Hsp90b1	LIINSL**Y**K	521.25257	Bromination (Y)	Y^{94}	HOBr
Heat shock protein HSP 90-beta - Hsp90ab1	SI**Y**YITGESK	619.75059	Bromination (Y)	Y^{484}	HOBr
Hypoxia up-regulated protein 1 - Hyou1	DAVI**Y**PILVEFTR	807.3823	Bromination (Y)	Y^{443}	HOBr
	YFQHLLGK	361.82556	Bromination (Y)	Y^{99}	HOBr
Laminin subunit alpha-1 - Lama1	ADNEVICTS**Y**YSK	814.30084	Bromination (Y)	Y^{192}	HOBr
	AKDCY**Y**DSSVAK	742.77172	Bromination (Y)	Y^{345}	HOBr
	DLI**Y**VGGLPHSK	459.54513	Bromination (Y)	Y^{2442}	HOBr; H_2O_2+Br
	GFGGQSCHQCSLG**Y**R	896.31991	Bromination (Y)	Y^{1088}	HOBr
	KHVI**Y**MDAPAPENGVR	625.61209	Bromination (Y)	Y^{1278}	HOBr
	KLYLGGLPSH**Y**R	494.56815	Bromination (Y)	Y^{2853}	HOBr
	L**Y**LGGLPSHYR	451.86983		Y^{2845}	
	KQGLLAVFDA**Y**DTSDKETK	736.33372	Bromination (Y)	Y^{2414}	HOBr
	SIGLWN**Y**IEREGK	548.24563	Bromination (Y)	Y^{2294}	HOBr
	SIGLWN**Y**IER	664.78529			
	TIDISNL**Y**IGGLPEDK	913.41452	Bromination (Y)	Y^{2630}	HOBr
	WHSI**Y**ITR	385.16447	Bromination (Y)	Y^{2212}	HOBr
	YFNSVSEK	526.19016	Bromination (Y)	Y^{1303}	HOBr
	YLIKENAK	352.82897	Bromination (Y)	Y^{1611}.	HOBr
Laminin subunit beta-1 - Lamb1	KCVCN**Y**LGTVK	710.29157	Bromination (Y)	Y^{1032}	HOBr
	CVCN**Y**LGTVK	646.24409			
	EGF**Y**DLSAEDPYGCK	914.82214	Bromination (Y)	Y^{445}	HOBr
	HNTKGLNCELCMDF**Y**HDLPWRPAEGR	659.67913	Bromination (Y)	Y^{316}	HOBr; H_2O_2+Br
	GLNCELCMDF**Y**HDLPWRPAEGR	938.71221			
	ISGVIGP**Y**RETVDSVEK	963.94398	Bromination (Y)	Y^{1216}	HOBr
	KAAQNSGEAE**Y**IEK	808.33353	Bromination (Y)	Y^{1671}	HOBr
	AAQNSGEAE**Y**IEK	744.28605			
	TLDGELDEK**Y**K	463.52417	Bromination (Y)	Y^{1698}	HOBr
	VV**Y**SVKQNADDVKK	557.59644	Bromination (Y)	Y^{1677}	HOBr
	YFQMSLEAEKR	493.86939	Bromination (Y)	Y^{1324}	HOBr; H_2O_2+Br
	YLEDKAQELVR	721.3197	Bromination (Y)	Y^{1753}	HOBr
	YVVLPRPVCFEK	792.86576	Bromination (Y)	Y^{663}	HOBr
	YYYAV**Y**DMVVR	760.29992	Bromination (Y)	Y^{263}	HOBr
Laminin subunit gamma-1 - Lamc1	ACACNP**Y**GTVQQQSSCNPVTGQCQCLPHVSGR	1233.8253	Bromination (Y)	Y^{887}	HOBr
	CDQCEENYF**Y**NR	888.76684	Deamidation (N); Bromination (Y)	Y^{1019}	HOBr
	FLGNQVLS**Y**GQNLSFSFR	719.31974	Deamidation (N); Bromination (Y)	Y^{571}	HOBr
	HNT**Y**GVDCEK	650.71675	Bromination (Y)	Y^{310}	HOBr
	LKD**Y**EDLREDMR	554.22602	Bromination (Y)	Y^{1305}	HOBr
	QDIAVISDS**Y**FPR	794.83571	Bromination (Y)	Y^{552}	HOBr
	S**Y**YYAISDFAVGGR	823.82789	Bromination (Y)	Y^{271}	HOBr
	FHTSRPESFAI**Y**KR	454.95868	Bromination (Y)	Y^{161}	HOBr
	K**Y**EQAKNISQDLEK	591.59487	Deamidation (N); Bromination (Y)	Y^{1234}	HOBr
Nidogen-2 - Nid2	**Y**AQTQHAYPGSR	486.19163	Bromination (Y)	Y^{974}	HOBr
	YVIGLEDHVGSNDQVFTYNGANLETCEHSHGR	925.13665	Deamidation (N); Bromination (Y)	Y^{486}	HOBr
Phosphoglycerate kinase 1 - Pgk1	SVVLMSHLGRPDGVPMPDK**Y**SLEPVAAELK	663.525	Bromination (Y)	Y^{76}	HOBr
	LGDV**Y**VNDAFGTAHR	571.5724	Bromination (Y)	Y^{161}	HOBr
Protein disulfide-isomerase A3 - Pdia3	ELNDFIS**Y**LQR	738.31187	Bromination (Y)	Y^{479}	HOBr
	LAPE**Y**EAAATR	635.25911	Bromination (Y) or 2	Y^{67}	HOBr
		674.21436	Bromination (Y)		
Serpin H1 - Serpinh1	L**Y**GPSSVSFADDFVR	908.31481	2 Bromination (Y)	Y^{134}	HOBr
SPARC – Sparc	LHLD**Y**IGPCK	431.84804	Bromination (Y)	Y^{144}	HOBr
Tissue-type plasminogen activator - Plat	**Y**IVHEEFDDDTYDNDIALLQLR	925.73098	Bromination (Y)	Y^{401}	HOBr
Tubulointerstitial nephritis antigen-like - Tinagl1	GVVSDNC**Y**PFSGR	768.28279	Bromination (Y)	Y^{292}	H_2O_2+Br

ECM isolated from PFHR9 cells was treated with 100 μM HOBr or with 100 μM H_2O_2 and 100 μM NaBr for 1 h and 30 min. Peptides with bromotyrosine (3-Br-Tyr) and/or di-bromotyrosine (3,5-Br-Tyr) were identified by data dependent acquisition mass spectrometry (DDA-MS). The identified group was considered when at least one sample of the 3 independent biological repeats contained detectable BrY-modified peptide.

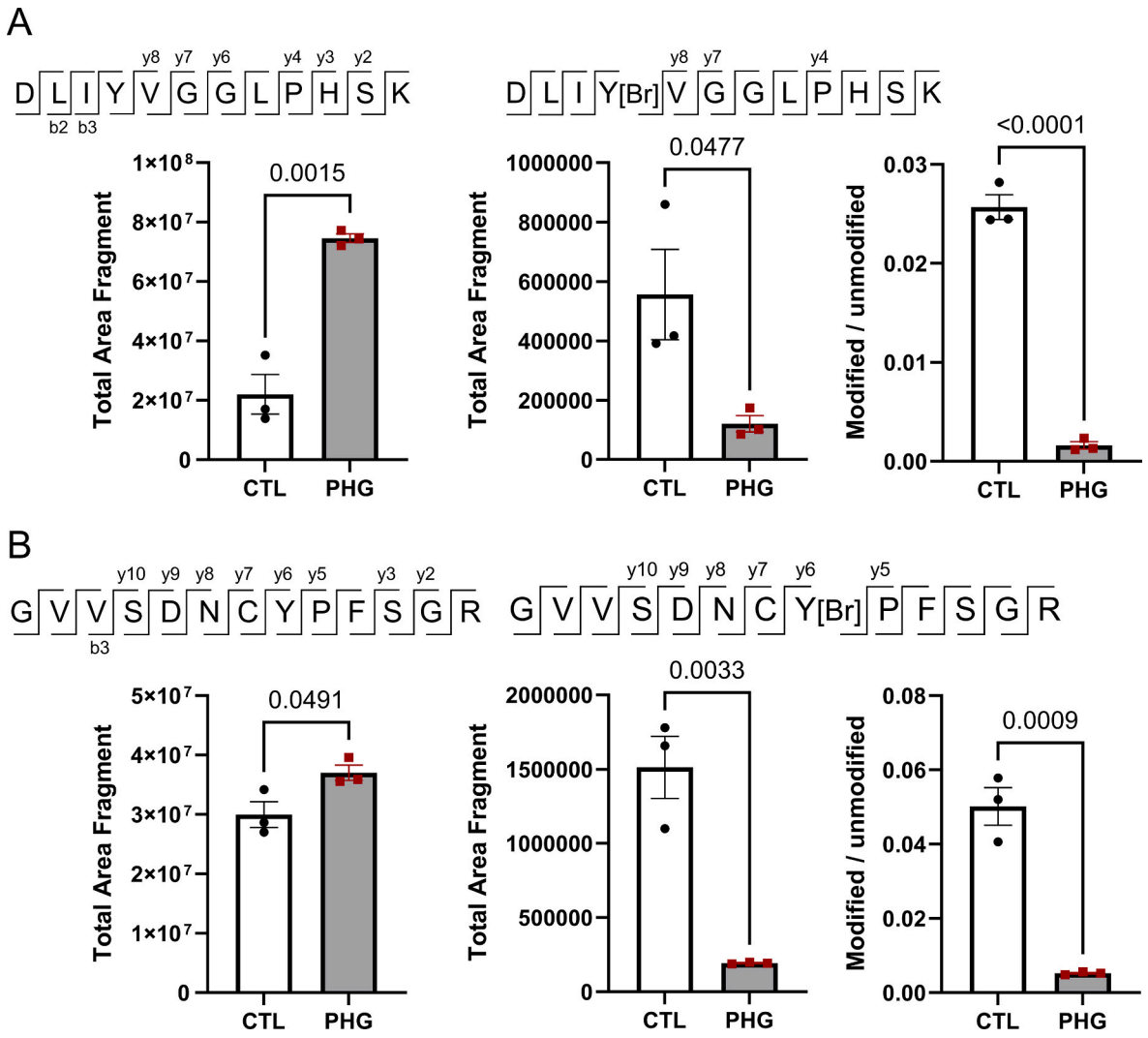

Fig. 1. PXDN mediates tyrosine bromination of basement membrane proteins. Confluent PFHR9 cells were grown for 6 days in the absence (CTL) or presence of PXDN inhibitor, phloroglucinol (PHG). Tryptic digests of ECM-enriched extracts were monitored by parallel reaction monitoring (PRM)-based targeted mass spectrometry. **A.** Quantification of fragment areas from unmodified laminin α1 (left - MS *m/z* 433.57497) and BrY-modified laminin α1 (middle - MS *m/z* 459.54513) peptide. **B.** Quantification of fragment areas from Tubulointerstitial nephritis antigen-like peptide, either unmodified (left - MS *m/z* 729.327563) or BrY-modified (middle - MS *m/z* 768.28279). Right panels represent ratios between the BrY-modified and unmodified peptide intensities. The total area fragment represents the sum of all peptide fragment (product ions) areas identified. Values are the mean of 3 independent biological repeats ± SEM. Differences among groups were evaluated by Student's T-test.

both cases markedly attenuated when cells were cultured in the presence of phloroglucinol (PHG), an irreversible inhibitor of PXDN. Peptide fragments spectra and masses from PRM samples are shown in Supplementary Fig. 2. Remarkably, tyrosine bromination of these proteins was not significantly enhanced after ECM incubation with H_2O_2/NaBr for 1.5 h (data not shown) indicating that this tyrosine bromination resulted primarily from endogenous production of H_2O_2 and trace amounts of bromide within the culture medium, in line with previous findings [5], and thus may represent a physiological process.

3.2. PXDN and laminin α1 are upregulated in bleomycin-induced pulmonary fibrosis in mice

Since fibrotic disease is typically associated with increased expression of ECM proteins and with upregulation of PXDN [20,21], we searched for BrY-modified ECM proteins in lung tissues from control mice and mice with experimentally-induced fibrosis. We first evaluated global alterations in lung ECM proteins, and observed overexpression of 83 ECM proteins in mouse lungs after bleomycin-induced fibrosis compared to control mice (Supplemental Fig. 3), 26 of which are BM proteins (Fig. 2), including various collagen IV α chains, several laminin α and β subunits, Tinagl1, lysyl oxidases, as well as Pxdn. To extend these proteomics results, we evaluated changes in expression of Pxdn and various BM proteins of interest during bleomycin-induced fibrosis, using RT-PCR, Western blot analysis, or immunofluorescence. No difference was found in lung tissue *Pxdn* mRNA expression between control and bleomycin-induced fibrosis (Fig. 3A), but overall Pxdn protein expression was significantly increased in bleomycin-induced fibrosis (Fig. 3B). Although full-length Pxdn protein has a molecular weight of around 165 kDa, the observed bands were in the range of 120–130 kDa,

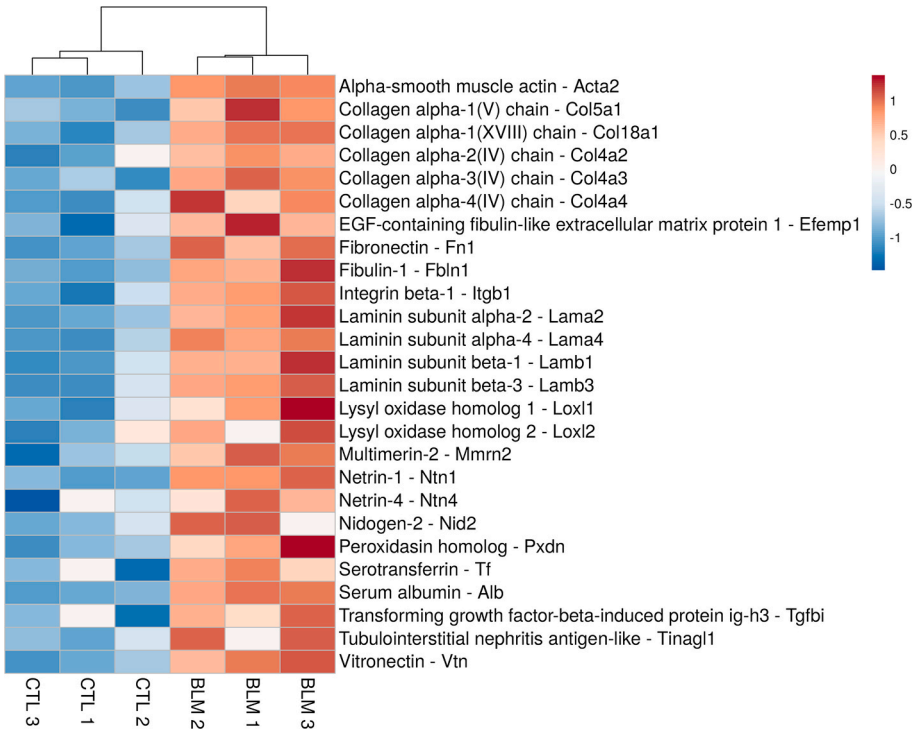

Fig. 2. Upregulation of BM proteins in mouse lung during bleomycin-induced fibrosis. C57BL6/NJ mice were treated with PBS (CTL) or 2.5 U/kg Bleomycin (BLM) and after 21 days the lung tissues were harvested and the ECM isolated. Proteins were identified by DDA proteomic analysis and label free quantitation (LFQ) intensities was used for statistic comparison. The intensity score indicates that the more towards the red color (score 1), the higher the protein expression. Values were obtained from 3 independent animals per group. Statistical comparison was performed by Student's T-test followed by Permutation-based FDR. All listed proteins were statistically different between groups ($p < 0.05$).

which likely resulted from a 30-kDa C-terminal proteolytic cleavage by proprotein convertase occurring prior to Pxdn extracellular release [31]. In addition, we evaluated mRNA expression of various BM proteins of interest, which showed significant increases in *Col4a2* mRNA in lung tissues of bleomycin-treated mice, but not of *Tinagl1* (Fig. 3C and D). Previous reports have linked changes in laminins with pulmonary fibrosis, most notably Lama1, which is normally absent from the adult lung but is increased during pulmonary fibrosis [32]. Indeed, *Lama1* mRNA and laminin α/β1 protein were both significantly increased in bleomycin-induced fibrosis (Fig. 3E and F), whereas we did not observe significant changes in *Lama3* (not shown), a major component of the alveolar BM [33].

Since ECM remodeling during pulmonary fibrosis is believed to depend largely on reciprocal interactions between activated (myo)fibroblasts and infiltrated monocyte-derived macrophages [34], we evaluated whether profibrotic activation of either cell type with the growth factor TGF-β1 would result in enhanced expression of PXDN and/or laminins. Indeed, both PXDN and *Lama1* mRNA and PXDN protein were overexpressed in human lung fibroblasts after TGF-β1 treatment (Fig. 4A–C). Moreover, TGF-β1 also induced mRNA expression of *Pxdn*, *Lama1* and *Lamb1* (Fig. 4D–F) as well as laminin α/β1 protein in mouse bone marrow-derived macrophages (Fig. 4G).

3.3. ECM proteins are tyrosine brominated in mouse lungs

Since Pxdn and additional BM proteins (such as laminin-1) were overexpressed in bleomycin-induced pulmonary fibrosis, we questioned whether there was a different pattern of protein tyrosine bromination in this disease model *in vivo*. We therefore evaluated the presence of BrY-modified proteins in ECM-enriched extracts of lung tissues from control and bleomycin-treated mice. As shown in Table 2, we detected 18 BrY-modified peptides among 11 proteins. Consistent with our studies of PHFR9 cells, the highest number of BrY-modified peptides represented laminins, with 8 different tyrosine site targets distributed among α3, β2 and γ1 subunits, accounting for 44% of the all identified BrY-modified peptides. Most detected brominated peptides (82%) represented BM proteins, including laminin subunits, collagens IV and VI, fibrillin-1, nephronectin, nidogen-2, and Tinagl1, suggesting that these modifications are largely due to localized secretion and activation of Pxdn within the BM. Importantly, the majority of BrY-modified peptides detected were observed in both control and bleomycin-treated mice, suggesting that these modifications may largely occur under physiological conditions. The DDA method is a stochastic sampling of proteomics and the missing identifications across samples can represent a missing at random (MAR). Thus, in order to compare identifications/intensities with accuracy, we selected the laminin peptides identified in DDA for a proteomic target mode (Supplemental Fig. 4). Fig. 5 shows the quantification of product ions from 5 laminin peptides that were identified as BrY-modified. This indicated that the extent of bromination ranged from 1.25% in Lamc1 to about 20% in Lama3, but was in neither case quantitatively different between control and bleomycin-treated mice. However, the remarkably prominent modification of Lama3 peptide SVDFGSTYSPWQYFAHSR (about 20%) and the Lamc1 peptide HNTYGVDCEK (about 15%), even in control lungs, is interesting and may point to a potential physiological role of such modifications.

3.4. ECM proteins are brominated in human lung tissues

To further extend our findings, we also investigated the presence of BrY-modified proteins in human lungs obtained from healthy control subjects or from patients with IPF. Two different sets of lung tissue samples were analyzed: (1) ECM-enriched fractions from randomly selected lung tissue regions; and (2) re-analysis of previously published proteomic data from decellularized lung tissues, either from whole lungs (wECM) or microdissected into airway (airECM), alveolar (aECM), and vascular (vECM) fractions [26]. The results of these analyses are

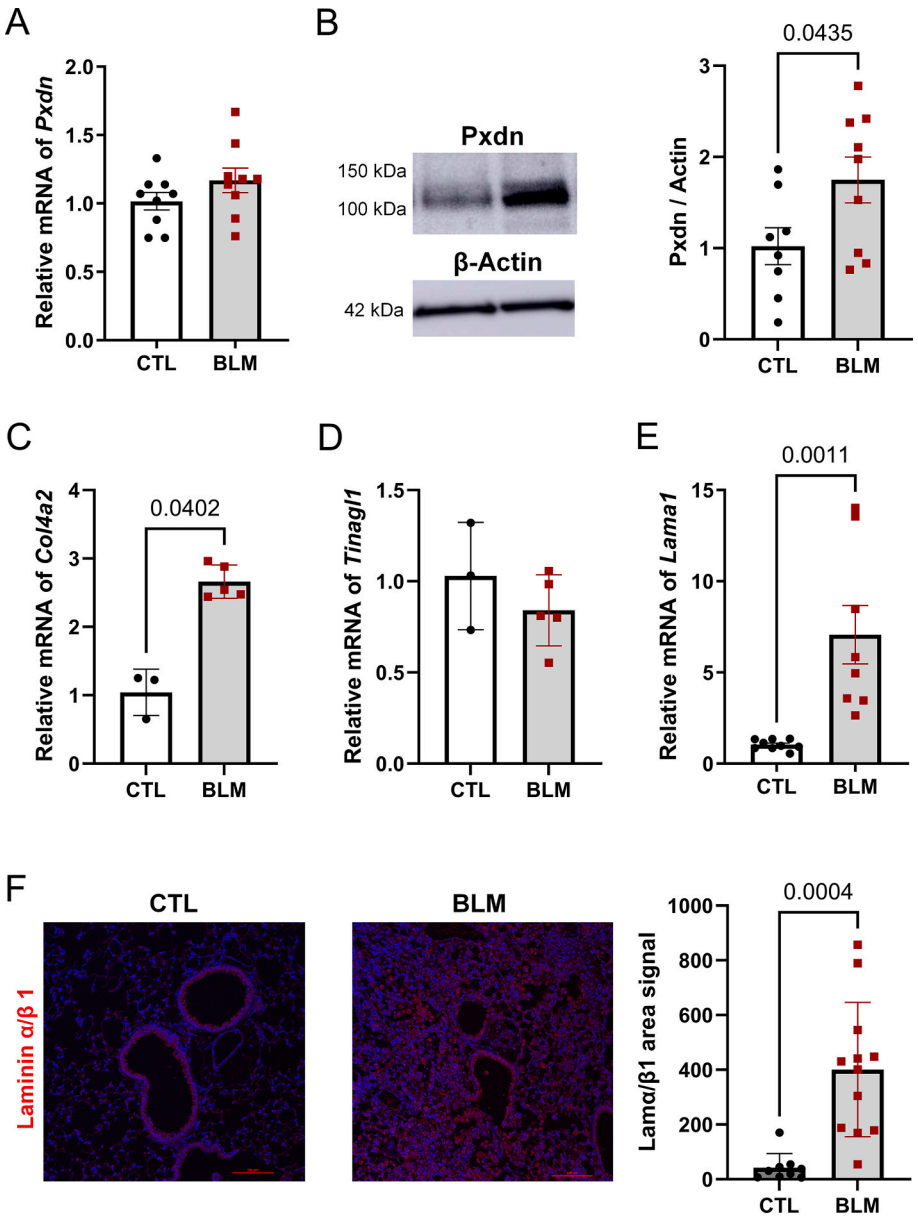

Fig. 3. PXDN and laminin α1 expression are increased in bleomycin-induced fibrosis. C57BL6/NJ (3 months) mice were treated with PBS (CTL) or 2.5 U/kg bleomycin (BLM) and after 21 days the lung tissues were harvested. **(A)** *Pxdn* mRNA and **(B)** Pxdn protein expression. **(C)** *Col4a2* and **(D)** *Tinagl1* mRNA expression. **(E)** *Lama1* mRNA and **(D)** laminin α/β1 protein expression. Immunofluorescence image of 20 × – scale bar: 100 μm. Values are the mean of at least 3 independent biological repeats ± SEM. Differences between groups were evaluated by Student's T-test.

presented in Tables 3 and 4. In total, we identified 7 BrY-modified peptides from 7 ECM proteins (Tables 3 and 4), 3 of which were common between both data sets: LSIIATDHTY^{209}RR from collagen VI α1, SVSIGY^{1490}LLVK from collagen IV α2, and GVVSDHCY^{293}PFSGR from TINAGL1. Interestingly, corresponding BrY-modified peptides were also detected in mouse lung tissues, i.e. LSIIATDHTY^{208}RR from collagen VI α1, SVSIGY^{1485}LLVK from collagen IV α2, and GVVSDHCY^{292}PFSGR from TINAGL1, and the latter was also found in ECM from cultured PFHR9 cells. These findings indicate that collagen IV α2, collagen VI α1, and TINAGL1 represent common targets for tyrosine bromination by PXDN in the lung, even under normal conditions, suggesting a possible physiological role for these modifications.

4. Discussion

Halogen modifications of biological molecules are increasingly recognized in various areas of biology, but its relevance for mammalian biology is still largely underappreciated. In this regard, and building on recent appreciation of bromine incorporation into ECM proteins related to PXDN activity [4,5], the main goal of the present study was to more deeply survey the possible ECM protein targets for HOBr and PXDN-mediated tyrosine bromination, as a post-translational modification that could affect ECM structure and interactions with adjacent cells. Laminins were identified as major targets for tyrosine bromination by HOBr or PXDN in PFHR9 cells. Laminins are heterotrimeric proteins composed of three different subunits: α (alpha), β (beta), and γ (gamma), with cell- or tissue-specific combinations of subunits related to their specific roles in different tissues and developmental stages. They represent the major noncollagenous proteins of BM and can bind directly to PXDN [35], consistent with the notion that laminins may be direct targets for PXDN-mediated modification. Recent studies from Davies and colleagues showed that laminin 111 is also a prominent target for tyrosine nitration [30] and chlorination [23] catalyzed by neutrophil myeloperoxidase. However, while myeloperoxidase is typically present

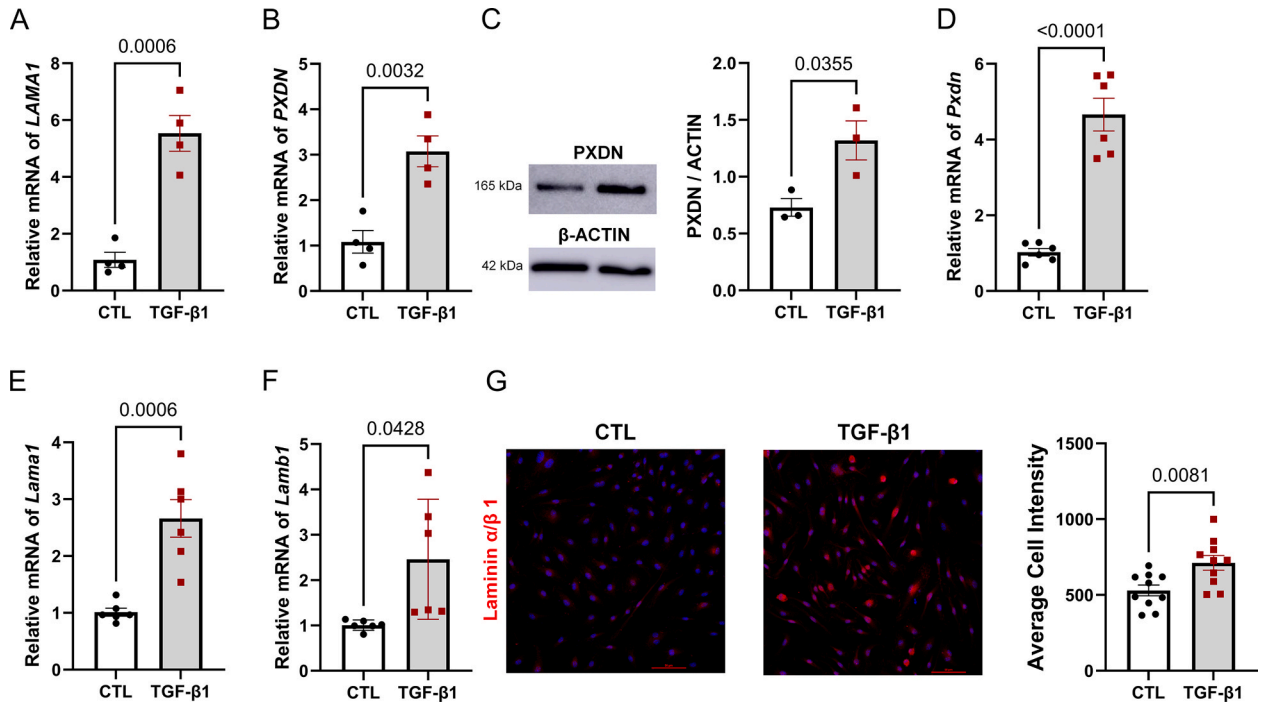

Fig. 4. PXDN and laminin expression are modulated in human lung fibroblasts (HLF) and bone-marrow-derived macrophages (BMDM) upon TGF-β1 stimulation. **(A–C)** HLFs were treated 5 ng/mL TGF-β1 for 48 h, and analyzed for *LAMA1* (A) or *PXDN* (B) mRNA or PXDN protein expression (C). **(D–G)** BMDM from C57BL6/NJ mice were treated 5 ng/mL TGF-β1 for 48 h, and analyzed for *Pxdn* **(D)**, *Lama1* **(E)**, or *Lamb1* **(F)** mRNA, or Laminin α/β1 protein expression by immunofluorescence imaging **(G).** Scale bar: 50 μm. Values are the mean of at least three independent biological replicates ± SEM. Differences among groups were evaluated by Student's T-test.

Table 2
ECM proteins are tyrosine brominated in mouse lungs.

Protein	Peptide	*m/z*	Variable modifications	Bromide Sites	Identified groups
Collagen alpha-1(VI) chain - Col6a1	LSIIATDHT**Y**RR	508.57033	Bromination (Y)	Y^{208}	CTL; BLM
Collagen alpha-2(IV) chain - Col4a2	SVSIG**Y**LLVK	578.78423	Bromination (Y)	Y^{1485}	CTL; BLM
Collagen alpha-3(VI) chain - Col6a3	VVIHFTDGADGDMADL**Y**R	696.94921 691.61757	Oxidation (M); Bromination (Y) or Bromination (Y)	Y^{1960}	CTL; BLM
Fibrillin-1 - Fbn1	G**Y**ILQEDGR	564.71962	Bromination (Y)	Y^{2476}	CTL
	YCKDINECETPGICMNGR	771.27438	Oxidation (M); Deamidation (N); Bromination (Y)	Y^{612}	BLM
Fibulin-5 - Fbln5	**Y**PGAYYIFQIK	720.81352	Bromination (Y)	Y^{374}	CTL
Laminin subunit alpha-3 - Lama3	SVDFGSTYSPWQ**Y**FAHSR	738.2956	Bromination (Y)	Y^{1833}	CTL
Laminin subunit beta-2 - Lamb2	DG**Y**SQQIVCQCR	796.28501	Bromination (Y)	Y^{949}	CTL; BLM
	D**Y**TGGEHCER	651.19618	Bromination (Y)	Y^{900}	CTL; BLM
	LP**Y**GGQCRPCPCPEGPGSQR	784.30864	Bromination (Y)	Y^{921}	CTL; BLM
Laminin subunit gamma-1 - Lamc1	HNT**Y**GVDCEK	650.71675	Bromination (Y)	Y^{310}	CTL; BLM
	LGNTEACSPCHCSPVGSLSTQCDS**Y**GR	1026.7197	Bromination (Y)	Y^{411}	BLM
	LHEATD**Y**PWRPALSPFEFQK	628.28392	Bromination (Y)	Y^{631}	BLM
	SQECYFDPEL**Y**R	842.80101	Bromination (Y)	Y^{356}	CTL; BLM
Nephronectin - Npnt	CHTGFDLM**Y**IGGK	531.5339	Oxidation (M); Bromination (Y)	Y^{205}	CTL
	DG**Y**EGDGLNCV**Y**IPK	889.3405	Bromination (Y)	Y^{246} or Y^{255}	CTL; BLM
Nidogen-2 - Nid2	ITQTAEGLDPEN**Y**LSIK	985.44127	Bromination (Y)	Y^{664}	BLM
Tubulointerstitial nephritis antigen-like - Tinagl1	GVVSDNC**Y**PFSGR	768.28279	Bromination (Y)	Y^{292}	CTL; BLM
	RGVVSDNC**Y**PFSGR	564.55799			

C57BL6/NJ mice were treated with PBS (CTL) or 2.5 U/kg Bleomycin (BLM) and after 21 days lung tissues were harvested and the ECM was isolated. Peptides with bromotyrosine (3-Br-Tyr) and/or di-bromotyrosine (3,5-Br-Tyr) were identified by DDA-MS. The identified group was considered when at least one sample of the 3 independent mice contained detectable BrY-modified peptide.

in extracellular regions during ongoing inflammatory conditions, PXDN is secreted into BM under physiological conditions to mediate collagen IV crosslinks as a normal feature of BM organization and tissue development [36]. Therefore, our observations of bromination on specific tyrosines in several laminins and in other BM proteins, including collagen IV α2, collagen VI α1, or Tinagl1, even in healthy mouse or human lung tissues, may reflect potentially physiologically relevant post-translational ECM modifications induced by PXDN that may affect BM function.

Although we did not directly establish PXDN as the key enzyme involved in tyrosine bromination of these BM proteins in the lung, and alternative peroxidases (e.g. MPO and EPO) may also be present (Supplemental Table 2), kinetic arguments [37–39] and the fact that PXDN is the main BM-associated heme peroxidase strongly support its main role

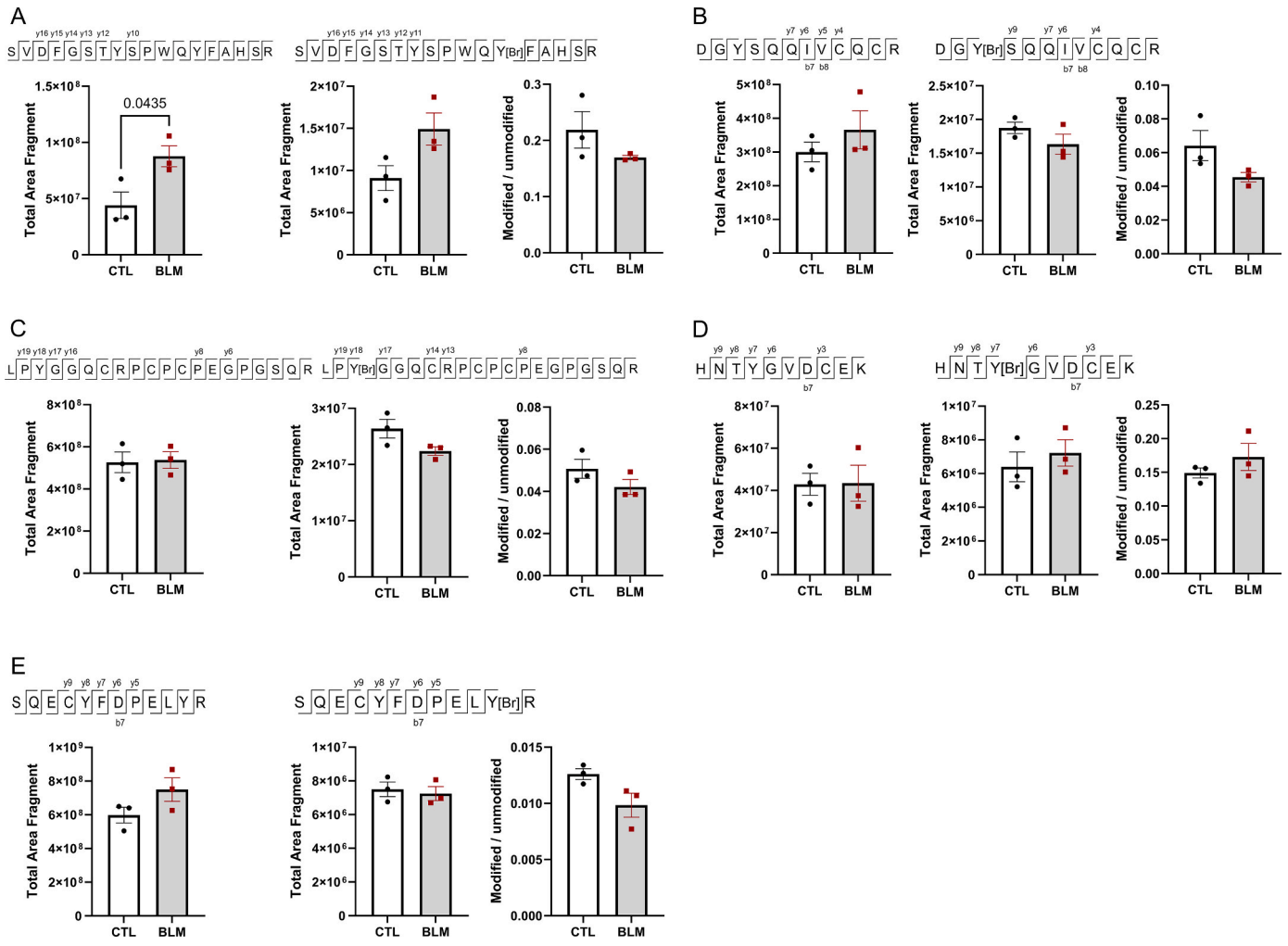

Fig. 5. Quantification of BrY-modified laminins in mouse lungs. C57BL6/NJ mice were treated with PBS (CTL) or 2.5 U/kg Bleomycin (BLM) for 21 days and lung ECM extracts were analyzed. Specific peptides were monitored by PRM-based targeted mass spectrometry. **(A)** Quantifications of fragment areas from unmodified (left – MS *m/z 712.32544*) and BrY-modified (middle – MS *m/z* 738.29561) laminin α3 peptide SVDFGSTYSPWQYFAHSR. **(B)** Quantifications of fragment areas from unmodified (left – MS *m/z* 757.32977) and BrY-modified (middle – MS *m/z* 796.28503) laminin β2 peptide DGYSQIVCQCR. **(C)** Quantifications of fragment areas from unmodified (left – MS *m/z 758*.33850) and BrY-modified (middle – MS *m/z* 784.30867) laminin β2 peptide LPYGGQCRPCPCPEGPGSQR. **(D)** Quantifications of fragment areas from unmodified (left – MS *m/z* 611.76151) and BrY-modified (middle – MS *m/z* 650.71676) laminin γ1 peptide HNTYGVDCEK. **(E)** Quantifications of fragment areas from unmodified (left -– MS *m/z* 803.84578) and BrY-modified (middle – MS *m/z* 842.80103) laminin γ1 peptide SQECYFDPELYR. Graphs on right side represent ratios between the BrY-modified and unmodified peptide intensities. The total area fragment represents the sum of all peptide fragment (product ions) areas identified. Values are the mean of 3 independent mice ± SEM. Differences among groups were evaluated by Student's T-test.

Table 3
ECM proteins are tyrosine brominated in human lung tissues.

Protein	Peptide	*m/z*	Variable modifications	Bromide Sites	Identified groups
Collagen alpha-1(VI) chain - COL6A1	LSIIATDHT**Y**RR	508.57033	Bromination (Y)	Y^{209}	CTL; IPF
Collagen alpha-2(IV) chain - COL4A2	SVSIG**Y**LLVK	578.78423	Bromination (Y)	Y^{1490}	CTL
Collagen alpha-3(IV) - COL4A3	ALEP**Y**ISR	513.71635	Bromination (Y)	Y^{1544}	CTL
Neutrophil defensin 1 - DEFA1	**Y**GTCI**Y**QGR	598.21365	Bromination (Y)	Y^{80} or Y^{85}	CTL; IPF
Tubulointerstitial nephritis antigen-like - TINAGL1	GVVSDHC**Y**PFSGR	520.19628	Bromination (Y)	Y^{293}	CTL

ECM was isolated from indistinct regions of healthy (CTL) and IPF lungs and peptides with bromotyrosine (3-Br-Tyr) and/or di-bromotyrosine (3,5-Br-Tyr) were identified by DDA-MS. The identified group was considered when at least one sample of the 3 independent subjects contained detectable BrY-modified peptide.

in ECM tyrosine bromination. During the preparation of the present manuscript, a similar study was published [40] in which the authors identified nidogen 2 and TINAGL1 as targets for PXDN-mediated bromination in ECM from mouse kidney glomeruli, largely consistent with our findings in lung tissues. Likewise, we found the same brominated nidogen 2 peptide in mouse lung tissue involving Y^{664}, pointing out this tyrosine site as a preferential target for PXDN. Additionally, the present study is the first one to demonstrate the presence of several other BrY-modified BM proteins in normal (mouse and human) lung tissues and also highlights laminins as major BM targets for PXDN-mediated bromination. Since laminin and nidogen establish high-affinity complexes within basement membranes [41], and nidogen also interacts with collagen IV and other components of the basement membrane, the ability of PXDN to brominate these various ECM proteins and cross-link collagen IV may depend strongly on PXDN binding to laminins or nidogen, thereby bringing PXDN into close proximity to collagen IV,

Table 4
ECM proteins are tyrosine brominated in specific anatomical human lung regions.

Protein	Peptide	*m/z*	Variable modifications	Bromide Sites	Identified groups
Collagen alpha-1(VI) chain - COL6A1	LSIIATDHT**Y**R LSIIATDHT**Y**RR	456.53663 508.57033	Bromination (Y)	Y^{209}	CTL-wECM, IPF - vECM
Collagen alpha-2(IV) chain - COL4A2	SVSIG**Y**LLVK	578.78423	Bromination (Y)	Y^{1490}	IPF - vECM
Dermatopontin - DPT	AGMEW**Y**QTCSNNGLVAGFQSR	1266.9309	Deamidation (N), 2 Bromination (Y)	Y^{103}	IPF - vECM
Fibrinogen beta chain - FGB	GTAGNALMDGASQLMGENRTMTIHNGMFFST**Y**DR	1274.5148	3 Oxidation (M); Deamidation (N); Brominatio (Y)	Y^{408}	IPF - aECM
Tubulointerstitial nephritis antigen-like - TINAGL1	GVVSDHC**Y**PFSGR	520.19628	Bromination (Y)	Y^{293}	IPF - wECM

Lung tissues from healthy (CTL) or IPF patients were decellularized, and whole decellularized lungs (wECM), alveolar-enriched ECM (aECM), airway ECM (airECM), and vasculature ECM (vECM) were prepared and analyzed as described in Hoffman et al. (2023). Peptides with bromotyrosine (3-Br-Tyr) and/or di-bromotyrosine (3,5-Br-Tyr) were identified by DDA-MS. The identified group was considered when at least 1 sample from 4 independent subjects contained detectable BrY-modified peptide.

even if collagen itself does not directly bind to PXDN [40].

The biological relevance of BM protein bromination is unclear, although some studies indicate that HOBr-induced ECM modification can reduce adhesion and proliferation of adjacent fibroblasts [9] or alter ECM fragmentation by proteases [42]. N-terminal domains of laminin chains ($\alpha\beta\gamma$) are required for efficient laminin polymerization [43], and the prominent brominated of laminin α3 on Y^{183} within its N-terminal domain might alter such polymerization. In this regard, a recent study indicated that tyrosine nitration of laminins interferes with their self-polymerization [30]. Similarly, an intriguing recent report demonstrated that genetically encoded incorporation of a single halotyrosine residue in prokaryotic filamentous cell-division protein (FtsZ) is sufficient to disrupt its self-organization [22]. Similar considerations may also apply to TINAGL1 (also known as adrenocortical zonation factor 1 [AZ-1], androgen-regulated gene 1 protein, or lipocalin 7), a BM protein that interacts with several matrix proteins and cell surface receptors, including laminin and collagen IV [44,45], and was consistently found to be brominated on a conserved tyrosine ($Y^{292/293}$) in each of our datasets. Lastly, Ivanov and colleagues [40] also reported that TINAGL1 and nidogen 2 can interact directly with PXDN and interfere with its binding to collagen IV. Collectively, these studies indicate that PXDN-mediated tyrosine bromination of these various BM proteins is likely related to its specific interactions with these various proteins, and may potentially serve a physiological role to regulate their functions, although this still awaits further study. In addition, a potential functional importance of tyrosine bromination is further supported by recent observations that a dehalogenase enzyme originally considered to specifically dehalogenate iodotyrosine to help salvage iodine to support thyroid hormone synthesis, IYD aka DEHAL1, is also capable of dehalogenating bromotyrosine [46].

A second question we attempted to address is whether alterations in PXDN in the context of pathological conditions such as cancer or fibrotic disease [16–21] would lead to corresponding increases in the extent of ECM protein bromination. However, we were unable to rigorously demonstrate quantitative alterations of bromotyrosine modifications of BM proteins in the context of experimentally-induced fibrosis in mice, for various potential reasons. A first limitation of our lung tissue analyses is the low sample size. Second, our analyses of mouse lung tissues were based on analysis of an entire lung lobe, whereas the presence of fibrosis in this bleomycin model is typically restricted to relatively small lung regions, with the remaining lung tissue appearing rather normal. Hence, any potential increases in bromination of BM proteins above normal levels would likely have been diluted by the abundant presence of normal non-involved lung tissue in our samples. Careful dissection and separation of fibrotic lung tissues from normal lung tissue would be more preferable to address this issue. Another confounding factor is that any increases in BrY-modified BM proteins (e.g. Col4a2, TINAGL1, etc.) may also be "diluted" by comparable increases in overall abundance of these ECM proteins in the context of fibrosis (e.g. Fig. 2). Lastly, it is possible that increases in PXDN expression during fibrosis may not be associated with corresponding increases in PXDN activity due to its potential oxidative inactivation [47]. More rigorous studies will be required to address these various possibilities, and to determine whether the overall degree of BM protein bromination or their distribution are altered during fibrosis in association with aberrant production and activation of PXDN, and whether this contributes to tissue remodeling. PXDN-generated HOBr can also induce alternative oxidative modifications, in addition to brominating tyrosine residues, such as bromination of tryptophan (Supplemental Table 3), or dityrosine cross-linking [48,49], which was found to be enhanced in fibrotic diseases such as IPF [50].

ECM remodeling during pathological conditions is also associated with altered expression of laminins [32,51,52]. Laminin α3 is a major component of alveolar BM, and although its overall expression may be enhanced in pulmonary fibrosis, its distribution is altered and laminin α3 was found to be lost in fibrotic lung regions in some cases [52]. In contrast, laminin α1, which is mostly absent in normal adult lung, was recently identified as a strong determinant of IPF pathogenesis. Laminin α1 can be produced by recruited macrophages and activated fibroblasts during fibrosis [32], both cell types playing reciprocal supportive roles in IPF pathogenesis [34], and our present study confirmed that PXDN and laminin α1 were both overexpressed in pro-fibrotically activated fibroblasts and macrophages, and in mouse lungs during bleomycin-induced fibrosis, in agreement with previous studies [19,21,32]. Despite the fact that laminin α1 was a major target for PXDN-mediated tyrosine bromination in PFHR9 cells, we were unable to detect BrY formation in laminin α1 in fibrotic lung tissues from mice or humans, possibly because its expression during fibrosis may be limited compared to other ECM proteins. Further directed studies using dissected fibrotic regions will likely be required to resolve this.

In summary, the present study highlights the involvement of PXDN in BrY modification of various BM proteins, in addition to its well-known role on collagen IV cross-linking. Since some of these tyrosine brominated proteins, e.g. laminins, collagen IV α2, collagen VI α1, and TINAGL1, are all able to closely interact with each other and with PXDN within the BM, their tyrosine bromination may exhibit some unknown biological function, which should be distinct from tyrosine bromination due to EPO-produced HOBr in inflammation. Lastly, increases in PXDN in the context of fibrotic disease, combined with increased expression of H_2O_2-generating enzymes that can fuel PDXN-mediated bromination, such as lysyl oxidases [53,54] or NADPH oxidases [55,56], may give rise altered incidence or distribution of tyrosine brominated ECM proteins, thereby potentially contributing to ECM remodeling in these pathological settings.

Funding

This study was supported by Fundação de Amparo à Pesquisa do Estado de São Paulo (FAPESP): CEPID Redoxoma 2013/07937-8; Young Investigator-2, grant number 2018/14898-2 (to F.C.M); and B.D. and L. C.C. received a scholarship from FAPESP. Work was also supported by NIH research grants R21 AG075491 (to A. v.d.V.) and R35 HL135828 (to Y.J.-H) and a research grant from the Department of Pathology and Laboratory Medicine at UVM (to L.C.C). Proteomics were performed at the Redox Proteomics Core of the Mass Spectrometry Resource at Chemistry Institute, University of São Paulo (FAPESP grant numbers 2012/12663-1, CEPID Redoxoma 2013/07937-8) led by Prof. Graziella Eliza Ronsein and Prof. Paolo Di Mascio, and at the Vermont Biomedical Research Network Proteomics Facility (RRID: SCR_018667) supported through NIH grant P20GM103449 from the INBRE Program of the National Institute of General Medical Sciences.

CRediT authorship contribution statement

Litiele Cezar Cruz: Writing – original draft, Methodology, Investigation, Funding acquisition, Data curation, Conceptualization. **Aida Habibovic:** Methodology, Investigation, Formal analysis. **Bianca Dempsey:** Methodology, Investigation, Data curation, Conceptualization. **Mariana P. Massafera:** Methodology. **Yvonne M.W. Janssen-Heininger:** Writing – review & editing, Funding acquisition, Formal analysis, Data curation. **Miao-chong Joy Lin:** Methodology, Data curation. **Evan T. Hoffman:** Resources, Methodology. **Daniel J. Weiss:** Resources, Methodology. **Steven K. Huang:** Resources, Methodology. **Albert van der Vliet:** Writing – review & editing, Supervision, Project administration, Investigation, Funding acquisition, Formal analysis, Data curation. **Flavia C. Meotti:** Writing – review & editing, Supervision, Resources, Project administration, Investigation, Funding acquisition, Formal analysis.

Declaration of competing interest

None

Data availability

Data will be made available on request.

Acknowledgments

The authors kindly thank Drs. Ying Wai Lam, Bin Deng, and Graziella Eliza Ronsein for their support and assistance with the mass spectrometry analyses, Miklós Geiszt for sharing anti-PXDN antibodies, and Drs. Christine Winterbourn and Martina Paumann-Page for scientific discussions related to PXDN and bromination chemistry.

Appendix A. Supplementary data

Supplementary data to this article can be found online at https://doi.org/10.1016/j.redox.2024.103102.

References

[1] S. Colon, P. Page-McCaw, G. Bhave, Role of hypohalous acids in basement membrane homeostasis, Antioxidants Redox Signal. 27 (2017) 839–854, https://doi.org/10.1089/ars.2017.7245.
[2] G. Bhave, C.F. Cummings, R.M. Vanacore, C. Kumagai-Cresse, I.A. Ero-Tolliver, M. Rafi, J.S. Kang, V. Pedchenko, L.I. Fessler, J.H. Fessler, B.G. Hudson, Peroxidasin forms sulfilimine chemical bonds using hypohalous acids in tissue genesis, Nat. Chem. Biol. 8 (2012), https://doi.org/10.1038/nchembio.1038.
[3] G.E. Ronsein, C.C. Winterbourn, P. Di Mascio, A.J. Kettle, Cross-linking methionine and amine residues with reactive halogen species, Free Radic. Biol. Med. 70 (2014) 278–287, https://doi.org/10.1016/j.freeradbiomed.2014.01.023.
[4] C. He, W. Song, T.A. Weston, C. Tran, I. Kurtz, J.E. Zuckerman, P. Guagliardo, J. H. Miner, S.V. Ivanov, J. Bougoure, B.G. Hudson, S. Colon, P.A. Voziyan, G. Bhave, L.G. Fong, S.G. Young, H. Jiang, Peroxidasin-mediated bromine enrichment of basement membranes, Proc. Natl. Acad. Sci. U. S. A. 117 (2020), https://doi.org/10.1073/pnas.2007749117.
[5] B. Bathish, M. Paumann-Page, L.N. Paton, A.J. Kettle, C.C. Winterbourn, Peroxidasin mediates bromination of tyrosine residues in the extracellular matrix, J. Biol. Chem. 295 (2020), https://doi.org/10.1074/jbc.ra120.014504.
[6] A. Pizzi, C. Pigliacelli, G. Bergamaschi, A. Gori, P. Metrangolo, Biomimetic engineering of the molecular recognition and self-assembly of peptides and proteins via halogenation, Coord. Chem. Rev. 411 (2020) 213242, https://doi.org/10.1016/j.ccr.2020.213242.
[7] G.W. Gribble, Naturally occurring organohalogen compounds, Acc. Chem. Res. 31 (1998) 141–152, https://doi.org/10.1021/ar9701777.
[8] T.J. Visser, Regulation of thyroid function, synthesis and function of thyroid hormones, 1–30, https://doi.org/10.1007/978-3-319-29195-6_1-1, 2018.
[9] M. Papanicolaou, P. He, S. Rutting, A. Ammit, D. Xenaki, D. van Reyk, B.G. Oliver, Extracellular matrix oxidised by the granulocyte oxidants hypochlorous and hypobromous acid reduces lung fibroblast adhesion and proliferation in vitro, Cells 10 (2021) 3351, https://doi.org/10.3390/cells10123351.
[10] H. Cai, C.Y. Chuang, S. Vanichkitrungruang, C.L. Hawkins, M.J. Davies, Hypochlorous acid-modified extracellular matrix contributes to the behavioral switching of human coronary artery smooth muscle cells, Free, Radic. Biol. Med. 134 (2019) 516–526, https://doi.org/10.1016/j.freeradbiomed.2019.01.044.
[11] A.S. McCall, C.F. Cummings, G. Bhave, R. Vanacore, A. Page-McCaw, B.G. Hudson, Bromine is an essential trace element for assembly of collagen IV scaffolds in tissue development and architecture, Cell 157 (2014) 1380–1392, https://doi.org/10.1016/j.cell.2014.05.009.
[12] L. Yang, Y. Bai, N. Li, C. Hu, J. Peng, G. Cheng, G. Zhang, R. Shi, Vascular VPO1 expression is related to the endothelial dysfunction in spontaneously hypertensive rats, Biochem. Biophys. Res. Commun. 439 (2013), https://doi.org/10.1016/j.bbrc.2013.09.012.
[13] H. Peng, L. Chen, X. Huang, T. Yang, Z. Yu, G. Cheng, G. Zhang, R. Shi, Vascular peroxidase 1 up regulation by angiotensin II attenuates nitric oxide production through increasing asymmetrical dimethylarginine in HUVECs, J. Am. Soc. Hypertens. 10 (2016), https://doi.org/10.1016/j.jash.2016.06.036.
[14] S.Y. Liu, Q. Yuan, X.H. Li, C.P. Hu, R. Hu, G.G. Zhang, D. Li, Y.J. Li, Role of vascular peroxidase 1 in senescence of endothelial cells in diabetes rats, Int. J. Cardiol. 197 (2015), https://doi.org/10.1016/j.ijcard.2015.06.098.
[15] Y. Yang, R. Shi, Z. Cao, G. Zhang, G. Cheng, VPO1 mediates oxidation of LDL and formation of foam cells, Oncotarget 7 (2016), https://doi.org/10.18632/oncotarget.9193.
[16] J. Dougan, O. Hawsawi, L.J. Burton, G. Edwards, K. Jones, J. Zou, P. Nagappan, G. Wang, Q. Zhang, A. Danaher, N. Bowen, C. Hinton, V.A. Odero-Marah, Proteomics-metabolomics combined approach identifies peroxidasin as a protector against metabolic and oxidative stress in prostate cancer, Int. J. Mol. Sci. 20 (2019), https://doi.org/10.3390/ijms20123046.
[17] A. Jayachandran, P. Prithviraj, P.H. Lo, M. Walkiewicz, M. Anaka, B.L. Woods, B. S. Tan, A. Behren, J. Cebon, S.J. McKeown, Identifying and targeting determinants of melanoma cellular invasion, Oncotarget 7 (2016), https://doi.org/10.18632/oncotarget.9227.
[18] M. Paumann-Page, N.F. Kienzl, J. Motwani, B. Bathish, L.N. Paton, N.J. Magon, B. Sevcnikar, P.G. Furtmüller, M.W. Traxlmayr, C. Obinger, M.R. Eccles, C. C. Winterbourn, Peroxidasin protein expression and enzymatic activity in metastatic melanoma cell lines are associated with invasive potential, Redox Biol. 46 (2021), https://doi.org/10.1016/j.redox.2021.102090.
[19] Z. Péterfi, Á. Donkó, A. Orient, A. Sum, Á. Prókai, B. Molnár, Z. Veréb, É. Rajnavölgyi, K.J. Kovács, V. Müller, A.J. Szabó, M. Geiszt, Peroxidasin is secreted and incorporated into the extracellular matrix of myofibroblasts and fibrotic kidney, Am. J. Pathol. 175 (2009) 725–735, https://doi.org/10.2353/ajpath.2009.080693.
[20] S. Colon, H. Luan, Y. Liu, C. Meyer, L. Gewin, G. Bhave, Peroxidasin and eosinophil peroxidase, but not myeloperoxidase, contribute to renal fibrosis in the murine unilateral ureteral obstruction model, Am. J. Physiol. Physiol. 316 (2019), https://doi.org/10.1152/ajprenal.00291.2018.
[21] M. Sojoodi, D.J. Erstad, S.C. Barrett, S. Salloum, S. Zhu, T. Qian, S. Colon, E. M. Gale, V.C. Jordan, Y. Wang, S. Li, B. Ataeinia, S. Jalilifiroozinezhad, M. Lanuti, L. Zukerberg, P. Caravan, Y. Hoshida, R.T. Chung, G. Bhave, G.M. Lauer, B. C. Fuchs, K.K. Tanabe, Peroxidasin deficiency Re-programs macrophages toward pro-fibrolysis function and promotes collagen resolution in liver, CMGH 13 (2022), https://doi.org/10.1016/j.jcmgh.2022.01.015.
[22] H. Sun, H. Jia, O. Kendall, J. Dragelj, V. Kubyshkin, T. Baumann, M.-A. Mroginski, P. Schwille, N. Budisa, Halogenation of tyrosine perturbs large-scale protein self-organization, Nat. Commun. 13 (2022) 4843, https://doi.org/10.1038/s41467-022-32535-2.
[23] T. Nybo, S. Dieterich, L.F. Gamon, C.Y. Chuang, A. Hammer, G. Hoefler, E. Malle, A. Rogowska-Wrzesinska, M.J. Davies, Chlorination and oxidation of the extracellular matrix protein laminin and basement membrane extracts by hypochlorous acid and myeloperoxidase, Redox Biol. 20 (2019) 496–513, https://doi.org/10.1016/j.redox.2018.10.022.
[24] B. Bathish, R. Turner, M. Paumann-Page, A.J. Kettle, C.C. Winterbourn, Characterisation of peroxidasin activity in isolated extracellular matrix and direct detection of hypobromous acid formation, Arch. Biochem. Biophys. 646 (2018) 120–127, https://doi.org/10.1016/j.abb.2018.03.038.
[25] V. Anathy, K.G. Lahue, D.G. Chapman, S.B. Chia, D.T. Casey, R. Aboushousha, J.L. J. van der Velden, E. Elko, S.M. Hoffman, D.H. McMillan, J.T. Jones, J.D. Nolin,

S. Abdalla, R. Schneider, D.J. Seward, E.C. Roberson, M.D. Liptak, M.E. Cousins, K. J. Butnor, D.J. Taatjes, R.C. Budd, C.G. Irvin, Y.-S. Ho, R. Hakem, K.K. Brown, R. Matsui, M.M. Bachschmid, J.L. Gomez, N. Kaminski, A. van der Vliet, Y.M. W. Janssen-Heininger, Reducing protein oxidation reverses lung fibrosis, Nat. Med. 24 (2018) 1128–1135, https://doi.org/10.1038/s41591-018-0090-y.

[26] E.T. Hoffman, F.E. Uhl, L. Asarian, B. Deng, C. Becker, J.J. Uriarte, I. Downs, B. Young, D.J. Weiss, Regional and disease specific human lung extracellular matrix composition, Biomaterials 293 (2023) 121960, https://doi.org/10.1016/j.biomaterials.2022.121960.

[27] M.C. McCabe, L.R. Schmitt, R.C. Hill, M. Dzieciatkowska, M. Maslanka, W. F. Daamen, T.H. van Kuppevelt, D.J. Hof, K.C. Hansen, Evaluation and refinement of sample preparation methods for extracellular matrix proteome coverage, Mol. Cell. Proteomics 20 (2021) 100079, https://doi.org/10.1016/j.mcpro.2021.100079.

[28] J. Rappsilber, M. Mann, Y. Ishihama, Protocol for micro-purification, enrichment, pre-fractionation and storage of peptides for proteomics using StageTips, Nat. Protoc. 2 (2007) 1896–1906, https://doi.org/10.1038/nprot.2007.261.

[29] V.F.S. Pape, H.A. Kovács, I. Szatmári, I. Ugrai, B. Szikora, I. Kacskovics, Z. May, N. Szoboszlai, G. Sirokmány, M. Geiszt, Measuring peroxidasin activity in live cells using bromide addition for signal amplification, Redox Biol. 54 (2022) 102385, https://doi.org/10.1016/j.redox.2022.102385.

[30] L.G. Lorentzen, C.Y. Chuang, A. Rogowska-Wrzesinska, M.J. Davies, Identification and quantification of sites of nitration and oxidation in the key matrix protein laminin and the structural consequences of these modifications, Redox Biol. 24 (2019) 101226, https://doi.org/10.1016/j.redox.2019.101226.

[31] S. Colon, G. Bhave, Proprotein convertase processing enhances peroxidasin activity to reinforce collagen IV, J. Biol. Chem. 291 (2016) 24009–24016, https://doi.org/10.1074/jbc.M116.745935.

[32] C.M. Lee, S.J. Cho, W.K. Cho, J.W. Park, J.H. Lee, A.M. Choi, I.O. Rosas, M. Zheng, G. Peltz, C.G. Lee, J.A. Elias, Laminin α1 is a genetic modifier of TGF-β1-stimulated pulmonary fibrosis, JCI Insight 3 (2018), https://doi.org/10.1172/jci.insight.99574.

[33] R.A. Pierce, G.L. Griffin, M. Susan Mudd, M.A. Moxley, W.J. Longmore, J.R. Sanes, J.H. Miner, R.M. Senior, Expression of laminin α 3 , α 4 , and α 5 chains by alveolar epithelial cells and fibroblasts, Am. J. Respir. Cell Mol. Biol. 19 (1998) 237–244, https://doi.org/10.1165/ajrcmb.19.2.3087.

[34] E. Setten, A. Castagna, J.M. Nava-Sedeño, J. Weber, R. Carriero, A. Reppas, V. Volk, J. Schmitz, W. Gwinner, H. Hatzikirou, F. Feuerhake, M. Locati, Understanding fibrosis pathogenesis via modeling macrophage-fibroblast interplay in immune-metabolic context, Nat. Commun. 13 (2022) 6499, https://doi.org/10.1038/s41467-022-34241-5.

[35] B. Sevcnikar, I. Schaffner, C.Y. Chuang, L. Gamon, M. Paumann-Page, S. Hofbauer, M.J. Davies, P.G. Furtmüller, C. Obinger, The leucine-rich repeat domain of human peroxidasin 1 promotes binding to laminin in basement membranes, Arch. Biochem. Biophys. 689 (2020), https://doi.org/10.1016/j.abb.2020.108443.

[36] K.E. Peebles, K.S. LaFever, P.S. Page-McCaw, S. Colon, D. Wang, A.M. Stricker, N. Ferrell, G. Bhave, A. Page-McCaw, Peroxidasin is required for full viability in development and for maintenance of tissue mechanics in adults, Matrix Biol. 125 (2024) 1–11, https://doi.org/10.1016/j.matbio.2023.11.005.

[37] P.G. Furtmüller, U. Burner, G. Regelsberger, C. Obinger, Spectral and kinetic studies on the formation of eosinophil peroxidase compound I and its reaction with halides and thiocyanate, Biochemistry 39 (2000) 15578–15584, https://doi.org/10.1021/bi0020271.

[38] M. Paumann-Page, R.-S. Katz, M. Bellei, I. Schwartz, E. Edenhofer, B. Sevcnikar, M. Soudi, S. Hofbauer, G. Battistuzzi, P.G. Furtmüller, C. Obinger, Pre-steady-state kinetics reveal the substrate specificity and mechanism of halide oxidation of truncated human peroxidasin 1, J. Biol. Chem. 292 (2017) 4583–4592, https://doi.org/10.1074/jbc.M117.775213.

[39] P.G. Furtmüller, U. Burner, C. Obinger, Reaction of myeloperoxidase compound I with chloride, bromide, iodide, and thiocyanate, Biochemistry 37 (1998) 17923–17930, https://doi.org/10.1021/bi9818772.

[40] S.V. Ivanov, K.L. Rose, S. Colon, R.M. Vanacore, B.G. Hudson, G. Bhave, P. Voziyan, Identification of brominated proteins in renal extracellular matrix: potential interactions with peroxidasin, Biochem. Biophys. Res. Commun. 681 (2023) 152–156, https://doi.org/10.1016/j.bbrc.2023.09.063.

[41] M. Dziadek, Role of laminin-nidogen complexes in basement membrane formation during embryonic development, Experientia 51 (1995) 901–913, https://doi.org/10.1007/BF01921740.

[42] M.D. Rees, T.N. McNiven, M.J. Davies, Degradation of extracellular matrix and its components by hypobromous acid, Biochem. J. 401 (2007) 587–596, https://doi.org/10.1042/BJ20061236.

[43] K.K. McKee, E. Hohenester, M. Aleksandrova, P.D. Yurchenco, Organization of the laminin polymer node, Matrix Biol. 98 (2021) 49–63, https://doi.org/10.1016/j.matbio.2021.05.004.

[44] T.A. Kalfa, J.D. Thull, R.J. Butkowski, A.S. Charonis, Tubulointerstitial nephritis antigen interacts with laminin and type IV collagen and promotes cell adhesion, J. Biol. Chem. 269 (1994) 1654–1659, https://doi.org/10.1016/S0021-9258(17)42077-1.

[45] T. Igarashi, Y. Tajiri, M. Sakurai, E. Sato, D. Li, K. Mukai, M. Suematsu, E. Fukui, M. Yoshizawa, H. Matsumoto, Tubulointerstitial nephritis antigen-like 1 is expressed in extraembryonic tissues and interacts with laminin 1 in the reichert membrane at postimplantation in the Mouse1, Biol. Reprod. 81 (2009) 948–955, https://doi.org/10.1095/biolreprod.109.078162.

[46] A. Phatarphekar, Q. Su, S.H. Eun, X. Chen, S.E. Rokita, The importance of a halotyrosine dehalogenase for Drosophila fertility, J. Biol. Chem. 293 (2018) 10314–10321, https://doi.org/10.1074/jbc.RA118.003364.

[47] S.V. Ivanov, K.L. Rose, S. Colon, B.G. Hudson, G. Bhave, P. Voziyan, Mechanism of peroxidasin inactivation in hyperglycemia: heme damage by reactive oxygen species, Biochem. Biophys. Res. Commun. 689 (2023) 149237, https://doi.org/10.1016/j.bbrc.2023.149237.

[48] C.L. Hawkins, M.J. Davies, The role of aromatic amino acid oxidation, protein unfolding, and aggregation in the hypobromous acid-induced inactivation of trypsin inhibitor and lysozyme, Chem. Res. Toxicol. 18 (2005) 1669–1677, https://doi.org/10.1021/tx0502084.

[49] G. Cheng, H. Li, Z. Cao, X. Qiu, S. McCormick, V.J. Thannickal, W.M. Nauseef, Vascular peroxidase-1 is rapidly secreted, circulates in plasma, and supports dityrosine cross-linking reactions, Free Radic. Biol. Med. 51 (2011) 1445–1453, https://doi.org/10.1016/j.freeradbiomed.2011.07.002.

[50] S. Blaskovic, Y. Donati, I. Ruchonnet-Metrailler, T. Seredenina, K.-H. Krause, J.-C. Pache, D. Adler, C. Barazzone-Argiroffo, V. Jaquet, Di-tyrosine crosslinking and NOX4 expression as oxidative pathological markers in the lungs of patients with idiopathic pulmonary fibrosis, Antioxidants 10 (2021) 1833, https://doi.org/10.3390/antiox10111833.

[51] J. Kropf, A.M. Gressner, A. Negwer, Efficacy of serum laminin measurement for diagnosis of fibrotic liver diseases, Clin. Chem. 34 (1988) 2026–2030, https://doi.org/10.1093/clinchem/34.10.2026.

[52] L.I. Morales-Nebreda, M.R. Rogel, J.L. Eisenberg, K.J. Hamill, S. Soberanes, R. Nigdelioglu, M. Chi, T. Cho, K.A. Radigan, K.M. Ridge, A.V. Misharin, A. Woychek, S. Hopkinson, H. Perlman, G.M. Mutlu, A. Pardo, M. Selman, J.C. R. Jones, G.R.S. Budinger, Lung-specific loss of α3 laminin worsens bleomycin-induced pulmonary fibrosis, Am. J. Respir. Cell Mol. Biol. 52 (2015) 503–512, https://doi.org/10.1165/rcmb.2014-0057OC.

[53] L. Chen, S. Li, W. Li, LOX/LOXL in pulmonary fibrosis: potential therapeutic targets, J. Drug Target. 27 (2019) 790–796, https://doi.org/10.1080/1061186X.2018.1550649.

[54] A. Poe, M. Martinez Yus, H. Wang, L. Santhanam, Lysyl oxidase like-2 in fibrosis and cardiovascular disease, Am. J. Physiol. Physiol. 325 (2023) C694–C707, https://doi.org/10.1152/ajpcell.00176.2023.

[55] R.A. Louzada, R. Corre, R. Ameziane El Hassani, L. Meziani, M. Jaillet, A. Cazes, B. Crestani, E. Deutsch, C. Dupuy, NADPH oxidase DUOX1 sustains TGF-β1 signalling and promotes lung fibrosis, Eur. Respir. J. 57 (2021) 1901949, https://doi.org/10.1183/13993003.01949-2019.

[56] L. Hecker, R. Vittal, T. Jones, R. Jagirdar, T.R. Luckhardt, J.C. Horowitz, S. Pennathur, F.J. Martinez, V.J. Thannickal, NADPH oxidase-4 mediates myofibroblast activation and fibrogenic responses to lung injury, Nat. Med. 15 (2009) 1077–1081, https://doi.org/10.1038/nm.2005.